JOURNAL OF MATERIALS SCIENCE 14 (1979) 1308–1320

The dielectic response of $K_x Al_x Ti_{8-x} O_{16}$ and $K_x Mg_{x/2} Ti_{8-x/2} O_{16}$

A. K. JONSCHER, K. L. DEORI
Department of Physics, Chelsea College, University of London, Pulton Place, London, UK
J.-M. REAU, J. MOALI
Laboratoire de Chimie du Solide du CNRS, 351 Cours de la Libération, 33405 Talence, France

Materials of the hollandite structure with the general formulae $K_x Al_x Ti_{8-x} O_{16}$ and $K_x Mg_{x/2} Ti_{8-x/2} O_{16}$ have been synthesized in the composition range $1.6 \leqslant x \leqslant 2.0$ and their dielectric properties have been measured in the temperature range 77 to 800 K and the frequency range 10^{-3} to 10^6 Hz. The observed response shows a whole range of features characteristic for both charge carrier and dipolar polarization processes and these are seen as being associated with the one-dimensional transport in channels in the hollandite structure. At low temperatures the dominant response is the "universal" dielectric relation in which the loss follows the law $\chi''(\omega) \propto \omega^{n-1}$, with the exponent $n < 1$ and equal specifically to approximately 0.7. This is followed at 120 to 180 K by a distinct loss peak superimposed on the above law, and finally at higher temperatures by a region of strong dispersion which is associated with strongly interacting many-body processes between charged carriers restricted by defects to move in limited regions of the channels.

1. Introduction

Solid electrolytes, otherwise known as fast ion conductors, have been receiving a considerable amount of attention in recent years on account of their remarkably high ionic conductivity with the attendant promise of applications, e.g. in solid batteries [1–4]. These materials also pose some very interesting questions with regard to the theory of transport of ions in solids, but more specifically, their dielectric response reveals certain unique features within the broader context of the dielectric response of solids [5–8].

It is possible to distinguish between three-, two- and one-dimensional ionic conductors, according to the easy directions of transport in them. In this way βPbF_2 is three-dimensional [9], while β-alumina is two-dimensional. As with one-dimensional electronic conductors [10], it is to be expected that the one-dimensional ionic conductors may show specific features of behaviour distinguishing them from the other two classes. The significant point is that a point-defect or obstacle to carrier motion has a much more dramatic effect in a one-dimensional system than in two- or three-dimensional systems.

A particular class of one-dimensional conductors in which K^+ ions move in well-defined unidirectional tunnels is represented by the materials of hollandite structure:

$$K_x Al_x Ti_{8-x} O_{16} \quad \text{and} \quad K_x Mg_{x/2} Ti_{8-x/2} O_{16}$$

with the composition range $1.6 < x < 2.0$, in both cases. The structure, preparation and the principal properties, such as the direct current (d.c.) conductivity, $\sigma_0(T)$ as function of temperature for these materials have been described by Réau *et al.* [11, 12]. These authors reported that $\sigma_0(T)$ at a given temperature increases with x in the Al series but decreases in the Mg series. At 600 K the increase between $x = 1.6$ and 2.0 is by a

TABLE I Values of the activation energy W_x (eV) depending upon the composition fraction x

	x				
	1.6	1.7	1.8	1.9	2.0
Al series	0.78	0.74	0.69	0.65	0.58
Mg series	0.80	0.88	0.97	1.07	1.18

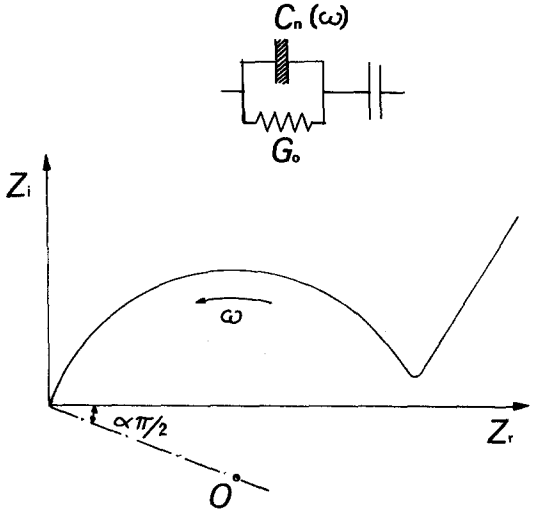

Figure 1 A schematic representation of the complex impedance diagram of a typical ionic conductor. The tilted circular arc corresponds to a "universal" capacitance $C_n(\omega)$ in parallel with a frequency-independent conductance G_0, the low-frequency "spur" arises from the presence of a series "barrier" capacitance. "O" represents the centre of the arc.

factor of 60 for Al and the corresponding decrease in Mg is by a factor of 100. It is clear, therefore, that the dominant factor is the mobility of the K^+ ions in the tunnels rather than their density. The mobility increases with increasing x in the Al solid solution and decreases with increasing x in the Mg solid solution.

The temperature dependence of the d.c. conductivity may be expressed by the relation

$$\sigma_0(T) = A \exp\left[-\frac{W_x}{k}\left\{\frac{1}{T}+\frac{1}{T_0}\right\}\right], \qquad (1)$$

where A and T_0 are constants, k is Boltzmann's constant and W_x is an activation energy which depends on the composition x. The form of Equation 1 implies that the pre-exponential factor depends on W_x in accordance with the generally applicable compensation rule [13]. The values of W_x given in Table I were reported.

2. Impedance measurements

Most electrical measurements on ionic conductors, including the determination of d.c. parameters, are, in fact, carried out by alternating current techniques using the complex impedance (Z) plots. The reason for this is that contact and interfacial phenomena make it difficult to determine the d.c. conductivity directly.

The complex Z plots for many materials have the form of well-defined circular arcs inclined to the horizontal at an angle $\alpha\pi/2$ falling typically in the range between 10° and 25° as shown schematically in Fig. 1. At sufficiently low frequencies this arc may go over into a well-defined inclined "spur" signifying the presence of a series contact barrier. Whereas the generally accepted interpretation of these inclined arc Z plots invokes some forms of distributions of "relaxation times", one of us has proposed an interpretation in terms of the same "universal" many-body mechanism as is found in a large number of other dielectric materials [6, 7, 14]. In this interpretation, the complex dielectric permittivity may be expressed by the following universal relation as function of the radian frequency, ω,

$$\begin{aligned}\epsilon(\omega) &= \epsilon'(\omega) - i\epsilon''(\omega) = \epsilon_\infty + a(i\omega)^{n-1} \\ &= \epsilon_\infty + a[\sin(n\pi/2) - i\cos(n\pi/2)]\,\omega^{n-1},\end{aligned} \qquad (2)$$

where ϵ_∞ is the limiting "high frequency" value of the permittivity and the exponent falls typically in the range $0 < n < 1$. The constant a determines the "strength" of the polarizability arising from the universal mechanism in question.

A characteristic feature of this "non-Debye" or universal relationship is that the ratio of the imaginary to the real parts of the dielectric susceptibility $\chi(\omega) = \epsilon(\omega) - \epsilon_\infty$ is independent of frequency:

$$\frac{\chi''(\omega)}{\chi'(\omega)} = \frac{\epsilon''(\omega)}{\epsilon'(\omega) - \epsilon_\infty} = \cot(n\pi/2). \qquad (3)$$

We note that this ratio is smaller than unity for $n > \frac{1}{2}$ and becomes larger than unity for $n < \frac{1}{2}$. The magnitude of the exponent n is associated in the many-body interpretation with the strength of particle–particle coupling, in the present instance the ion–ion coupling, small values of n corresponding to strongly interacting systems [7].

The somewhat limited range of data published by Réau *et al.* [12] gives strongly inclined arcs

which are not well-developed on the low-frequency side and do not show any sharply defined transition into the spur region, in marked contrast with, for instance, the response of β-PbF_2 [9]. The value of n derived from these data is approximately 0.7.

The data reported in the present paper were taken partly at Bordeaux and partly at Chelsea, the respective ranges of temperature and frequency being: Chelsea 10^{-4} to 10^{4} Hz, 77 to 373 K, Bordeaux 5 to 10^{6} Hz, 473 to 873 K. The samples were prepared at Bordeaux by the same methods as described earlier. The measurements by the Bordeaux group were carried out using a Hewlett–Packard 3575 A impedance meter with the samples placed in a furnace with inert gas atmosphere.

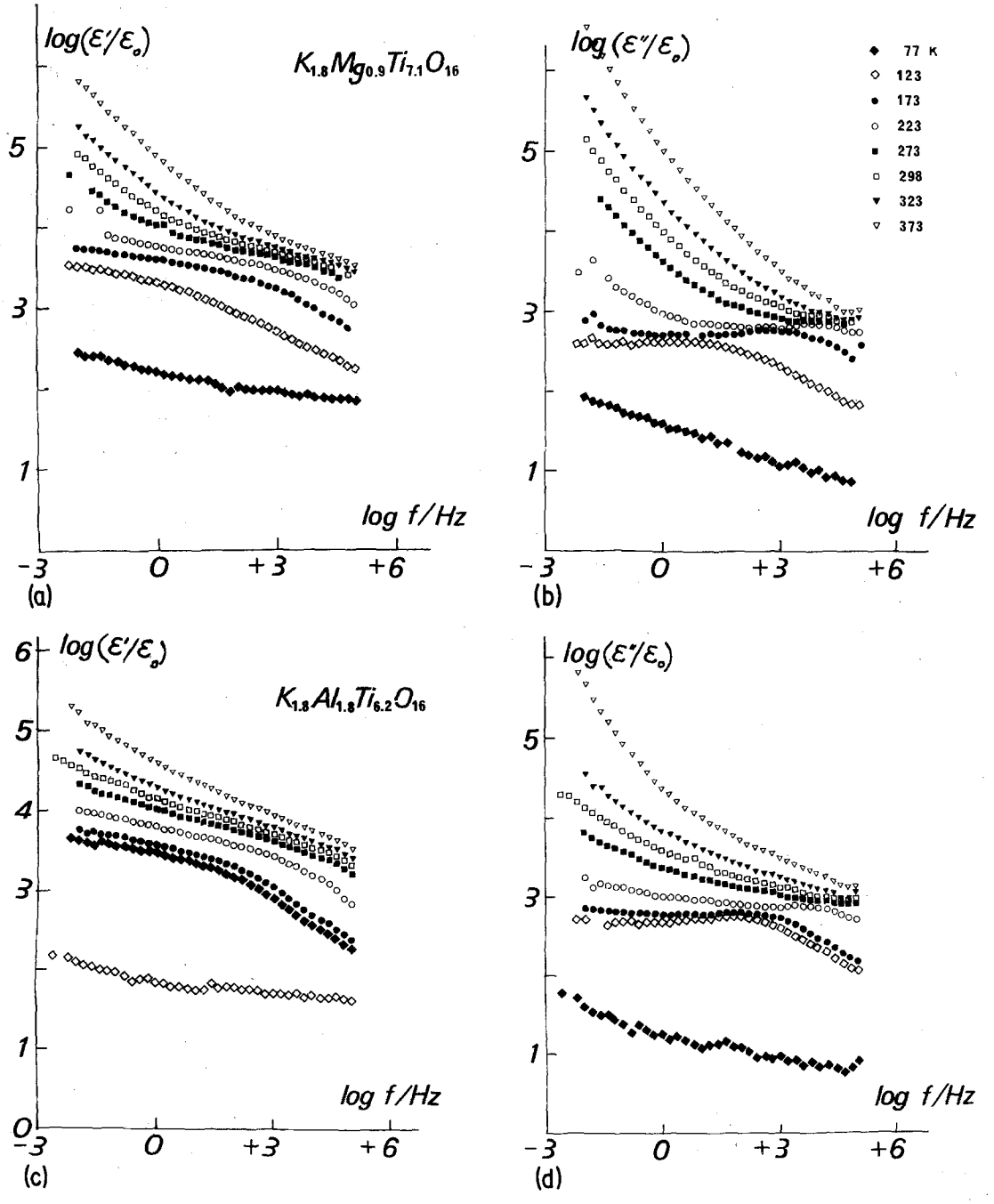

Figure 2 The frequency dependence of the real and imaginary parts of the relative permittivity, $\epsilon_r = \epsilon/\epsilon_0$, over the lower range of temperatures for one sample each of the Mg and Al series with $x = 1.8$.

The Chelsea group were using their Solartron 3381 automatic frequency response analyser (FRA) with automatic data recording and display [15]. We have established a good consistency of results between the two laboratories.

The following compositions were investigated, the Bordeaux and Chelsea groups using separate samples prepared in the same runs:

Al series x = 1.6, 1.7, 1.8, 1.9, 2.0

Mg series x = 1.6, 1.7, 1.8, 1.9, 2.0.

3. Low-temperature measurements

The low-frequency and low-temperature data for the composition $x = 1.8$ for both Al and Mg hollandites are presented in Fig. 2 as plots of $\epsilon'(\omega)$ and $\epsilon''(\omega)$ for a range of temperatures. The loss data for the Mg sample show a perfect example of the universal behaviour at 77 K with a value of the exponent $n = 0.97$, while those for the Al sample show a similar behaviour with a slight increase of slope towards low frequencies, signifying the influence of a more dispersive mechanism there. The corresponding $\epsilon'(\omega)$ data show clear influence of ϵ_∞ at high frequencies, with a value of the exponent $n = 0.87$, while those for the Al sidered quite reasonable for this type of material.

At 123 and 173 K both samples show clear loss peaks superimposed on the same general universal trend, with corresponding dispersion of $\epsilon'(\omega)$. The low-frequency values of $\epsilon'(\omega)$ now reach 3 to 5 x 10^3, values which cannot reasonably be attributed to lattice polarizability. The peaks are much more pronounced in the Al samples, and it is interesting to note that the spread of values of the loss peaks is also larger between the various compositions than in the corresponding Mg series. This is shown in Fig. 3, where the amplitudes of the peaks are seen to grow in the sequence $x = 2.0 \rightarrow 1.6 \rightarrow 1.8 \rightarrow 1.7 \rightarrow 1.9$. By contrast, in the Mg series the peaks at 123 K are very closely spaced, while the 77 K loss data are equally narrowly spread as for Al.

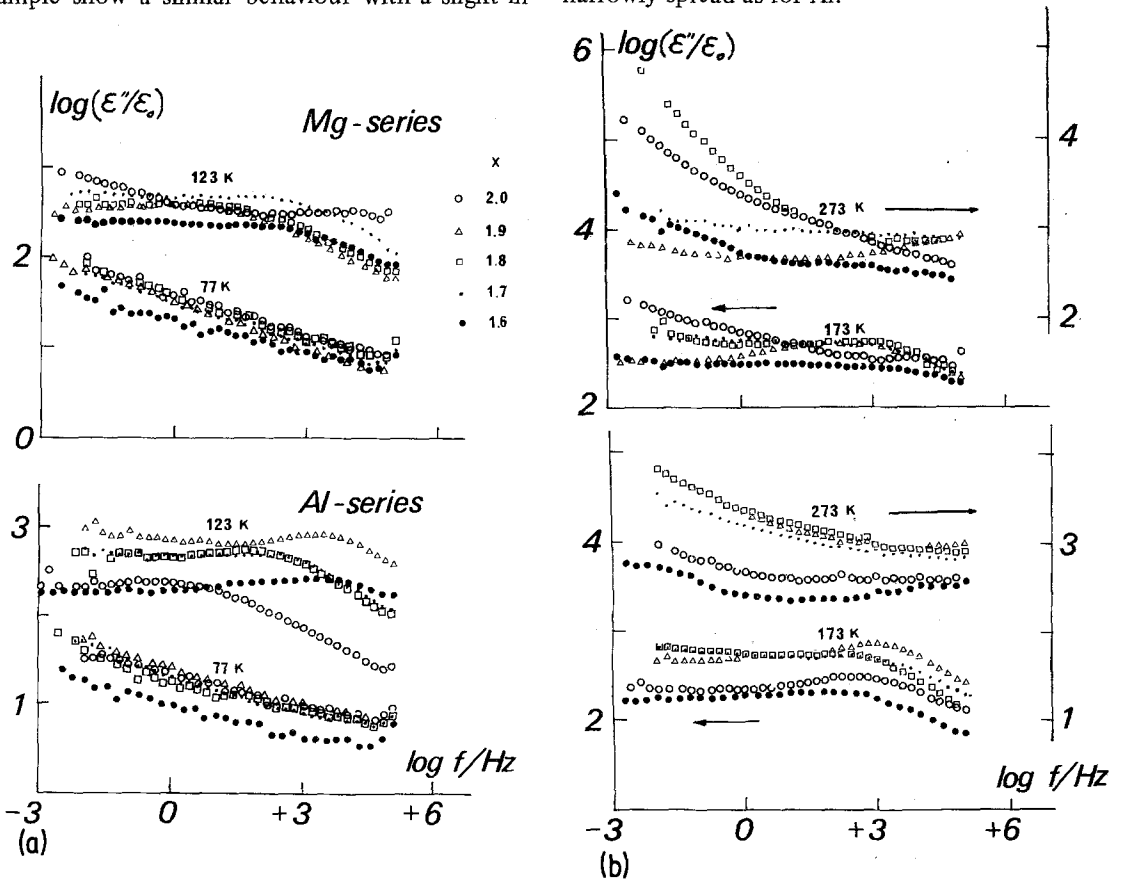

Figure 3 The frequency dependence of the dielectric loss at 77, 123, 173 and 273 K for the entire range of composition of both Mg and Al series. The meaning of the symbols is the same in all four diagrams. Note the separate ordinate scales for the higher temperatures.

With a further rise in temperature we find a rapid increase of both $\epsilon'(\omega)$ and $\epsilon''(\omega)$, the Mg series showing a steeper rise, with smaller values of the exponent n than the Al series, but in both cases $n < \frac{1}{2}$ is attained at the highest temperature of 373 K. The sequences of rising values of both $\epsilon'(\omega)$ and $\epsilon''(\omega)$ at constant low frequencies for different compositions are $2.0 \rightarrow 1.7 \rightarrow 1.8 \rightarrow 1.9$ for Al and $1.9 \rightarrow 1.7 \rightarrow 1.6 \rightarrow 2.0 \rightarrow 1.8$ for Mg series.

While the details of the low-temperature behaviour across the composition range are somewhat complicated, there remain a few clear-cut features which may be summarized as follows:

(i) three types of dielectric behaviour are clearly discernible, namely the classic universal behaviour given by Equation 2 at 77 K, a loss peak in the intermediate temperature range and a strong low-frequency dispersion at 300 K and above;

(ii) the real and imaginary parts of permittivity attain values which at the higher temperatures are completely incompatible with any form of lattice polarization and must, therefore, be attributable either to some form of spurious barrier phenomena or to the presence of charge carriers;

(iii) the dielectric response seems to be practically independent of x in the two solid solutions.

We shall return to a detailed discussion of the implications of this behaviour in a later section.

4. High-temperature measurements

One of the immediately striking features of the dielectric response of hollandites at temperatures above 500 K is the shape of the complex Z diagrams which become very broad and depart strongly from the classical inclined circular arc shape with a clearly distinguishable low-frequency spur. Fig. 4 shows typical examples of this type of response which is not compatible with any form of series combination of two different regions, such as the bulk and the barrier.

This behaviour may be understood in terms of the frequency dependence of the real and imaginary components of the complex permittivity. Figs. 5 and 6 show the data for $\epsilon'(\omega)$ and $\epsilon''(\omega)$ in the upper temperature region for one example each from the Mg and Al series, respectively. The onset of a strong low-frequency dispersion for both the real and the imaginary parts is evident, with the characteristic feature that their ratio remains approximately independent of frequency. This is seen more clearly in the compilation of Fig. 7 which gives the data for $\epsilon'(\omega)$ and $\epsilon''(\omega)$ plotted in pairs for the highest available temperature for every composition in the two series. The dielectric loss follows the law of Equation 2 but with the values of the exponent n close to zero. The chain-dotted lines give the expected position of the real part $\epsilon'(\omega)$ calculated from the Kramers–Kronig relation (Equation 3) with the appropriate

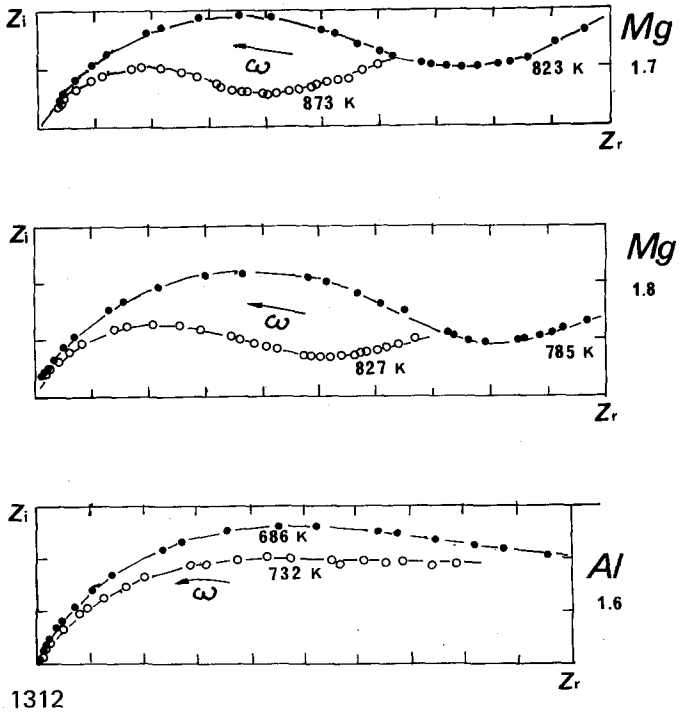

Figure 4 The complex impedance (Z) diagrams for two Mg samples with $x = 1.7$ and 1.8 and for an Al sample with $x = 1.6$. These plots refer to the higher range of temperatures and they show clearly the strong departure from the more commonly found circular arc plots with a separate low-frequency part representing the effect of a separate barrier, as shown in Fig. 1.

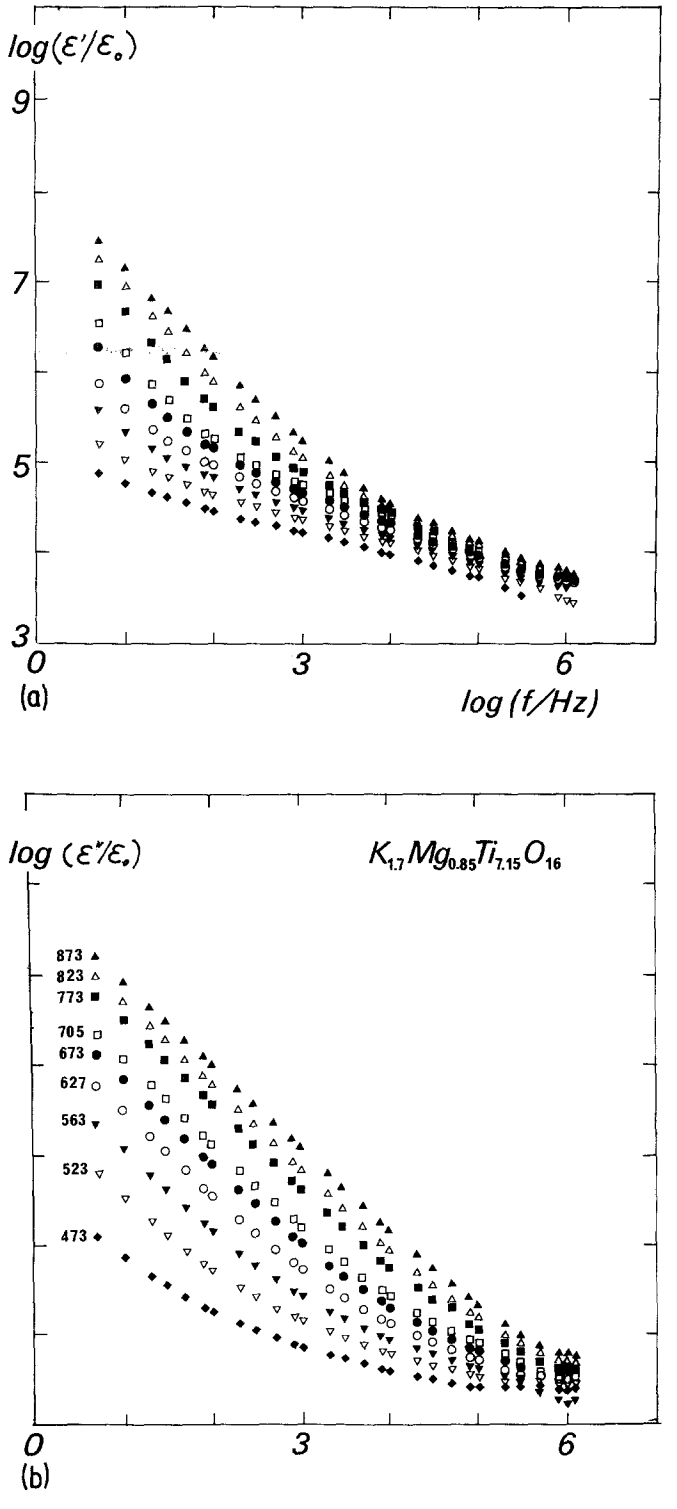

Figure 5 The complete set of data for the frequency dependence of the real and imaginary components of the complex permittivity in the higher range of temperatures for a sample of $K_{1.7}Mg_{0.85}Ti_{7.15}O_{16}$ composition. Note the strong low-frequency dispersion gradually replacing the flatter frequency response characterizing the lower temperature behaviour and also the very high values of the permittivity attained at the lowest frequencies.

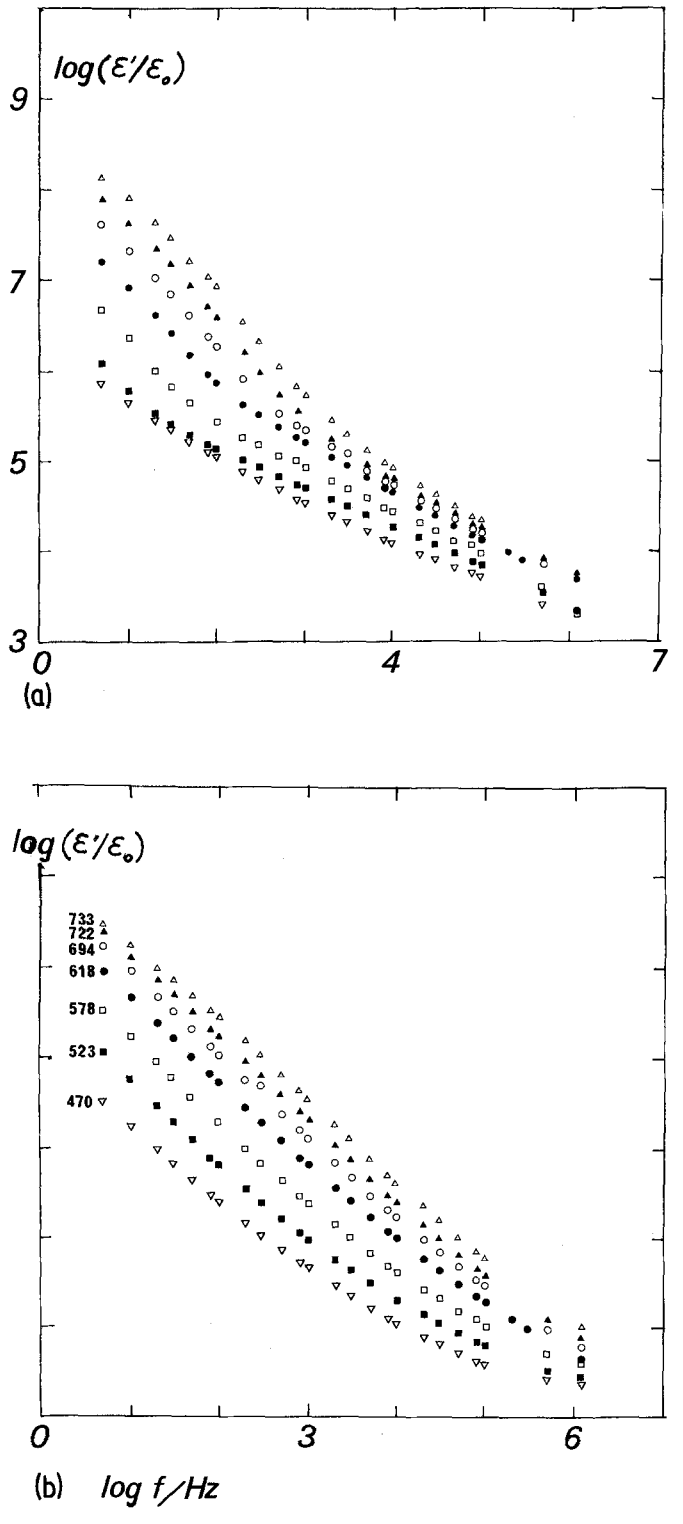

Figure 6 Corresponding plots to Fig. 5 relating to a sample of $K_2Al_2Ti_6O_{16}$ composition. Note the stronger dispersion at low frequencies.

value of n. The agreement is seen to be excellent in some cases, while in others the graph of $\epsilon'(\omega)$ shows a bulge with only gradual attainment of parallelism, seen especially in the Al samples. On closer inspection we note that the $\epsilon''(\omega)$ data in these cases show a distinct change of slope towards higher values of n at the lowest frequencies and this necessitates a reduction of the ratio $\epsilon''(\omega)/\epsilon'(\omega)$, as seen experimentally. This ratio is a more sensitive indicator of the value of n than the slope of the graph in the region of small values of n.

Figs. 5 and 6 show very clearly the gradual transition from the low-temperature universal response with values of n in the range 0.6 to 0.7, to the high-temperature strongly dispersive regime with small values of n. This transition had already been apparent in Fig. 2 but is now much more fully developed.

A different aspect of this behaviour may be seen in Fig. 8 where the data for the Mg sample $x = 1.8$ and Al sample $x = 2$ are shown in the "normalized" form obtained by translating the data for different temperatures laterally to bring them into coincidence. This technique can be very effective where there is a single mechanism of polarization [7] but if more than one mechanism is at play, it may be difficult to obtain the optimal fit for both $\epsilon'(\omega)$ and $\epsilon''(\omega)$ in the low-frequency region, giving rise to some discrepancies at the higher frequencies. The locus of the translation vector gives a good straight line plot against $1/T$ for the Mg sample, with an activation energy of 0.95 eV, but the Al sample does not give such a clear-cut activation response. It should be noted that the normalized graphs for ϵ' and ϵ'' have been displaced with respect to one another in the interest of clarity, since

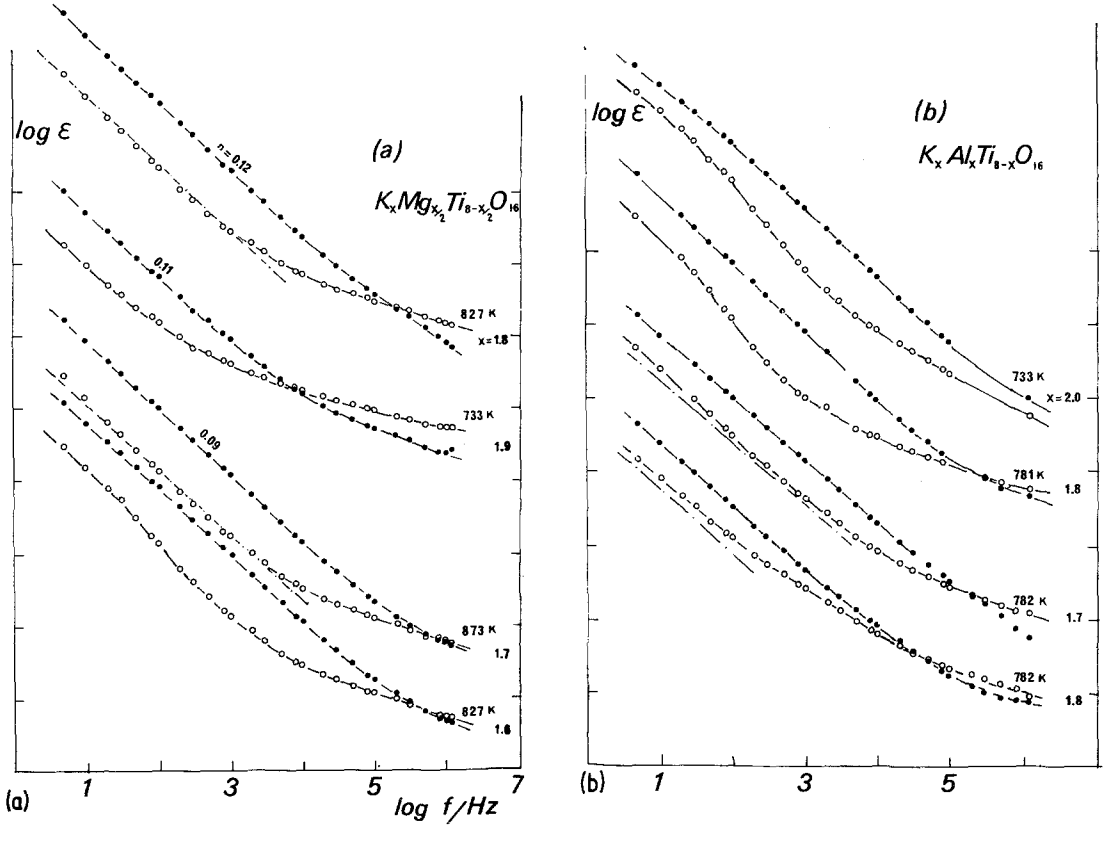

Figure 7 A compilation of the frequency dependence data at the highest available temperature for each of the compositions in the Mg and Al series. The real part ϵ' is always denoted by open circles and the imaginary part ϵ'' by solid circles and the respective pairs are on a common ordinate axis, while different pairs are successively displaced vertically by one decade, to avoid undue overlapping. The values of the exponent n indicated in the diagrams are obtained from the low-frequency parts of the ϵ'' plots and the chain-dotted lines are then drawn at the Kramers–Kronig compatible separation to indicate the theoretically expected position of the real part ϵ'. This was not done for the upper two Al samples which show two slopes in the ϵ'' graph and the corresponding bulge in the ϵ' plot.

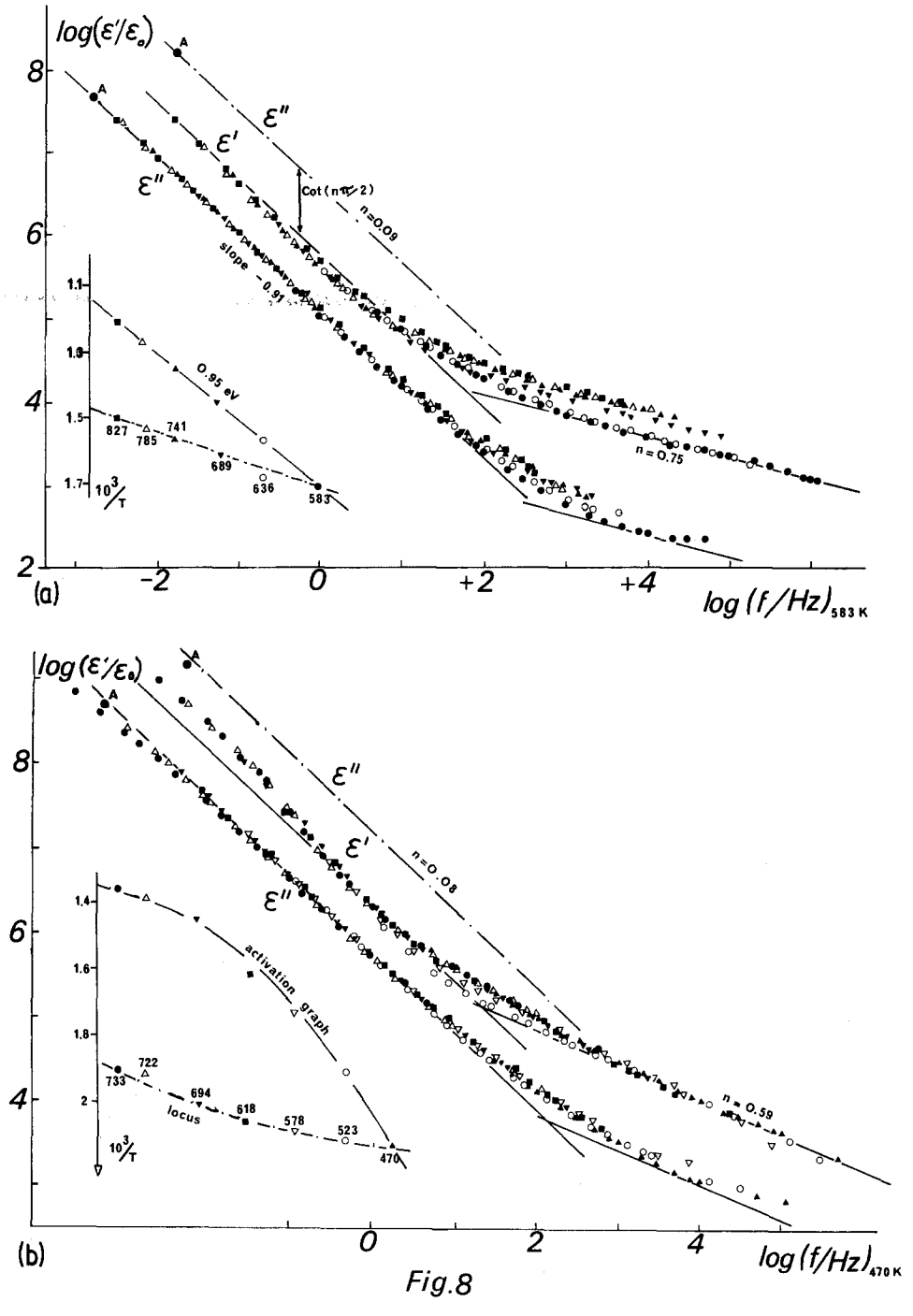

Fig.8

Figure 8 Normalization of the $\epsilon'_r(\omega)$ and $\epsilon''_r(\omega)$ data for different temperatures for the Mg sample $x = 1.8$ and the Al sample $x = 2.0$. The normalization was carried out to obtain the best fit of both the real and the imaginary components in the lower part of the frequency range, and some straggling of data is visible at the higher frequencies, especially in the Mg sample, indicating that the high- and low-frequency mechanisms are not the same. The normalization was carried out by lateral shifting of the data for the different temperatures, the locus of a representative point is shown in each case. The corresponding frequency shift is then plotted agains $1/T$ in the insets, to reveal the temperature dependence. The Mg sample gives a clear activation energy of 0.95 eV, the Al sample shows no such simple relation. In order to avoid confusing overlapping the ϵ'_r and ϵ''_r data were displaced laterally and the chain-dotted lines in each case indicate the theoretical position of ϵ''_r with respect to ϵ'_r. The points A denote the corresponding positions on the displaced diagrams. The frequency scale refers to the $\epsilon'_r(\omega)$ data at the respective lowest temperatures.

they tend to intersect one another, as in Fig. 7. The chain-dotted line represents the proper position of ϵ'' relative to ϵ' with the point "A" giving the correct relative positions on the displaced graphs. 0.95 eV is the same as the d.c. activation energy in Table I for the Mg compound.

Finally, in Fig. 9 we look at the temperature dependence of the ϵ' and ϵ'' at the lowest frequency, $f = 5$ Hz, for all compositions in the two series. This representation provides information about the activation energies at constant frequency, as well as the relative magnitudes of the dielectric permittivity in the low-frequency, high-temperature regime. It is now instructive to compare the information on Fig. 9 with that on Figs. 5 and 6. The latter represent the complete $\epsilon(\omega, T)$ responses for one particular composition, the former gives the relative values of $\epsilon''(T)$ at 5 Hz for the different samples. The activation plots of Fig. 9 give reasonably well-defined activation energies in the range 0.5 to 0.7 eV which are significantly lower than the d.c. activation energies given in Table I and also lower than the energy obtained from the frequency shift in the normalization operation shown in Fig. 8. This discrepancy is not surprising if we note the fact that the direct current and dielectric polarization are independent processes which reflect different physical situations, but in addition it is relevant to note that the temperature dependence at constant frequency shown in Fig. 9 is not the most reliable way of ascertaining the activation energy of a dielectric process – a much more satisfactory way in general is the plot of frequency shift in the normalization process.

The important information to be obtained from Fig. 9 concerns the dependence of the dielectric loss on the composition of the samples; it is clear that the dependence is much stronger in the Al series than in the Mg series, with the sequence of increasing loss

$$\text{Al } x = 1.6 \rightarrow 1.7 \rightarrow 1.8 \rightarrow 2.0$$

$$\text{Mg } x = \quad \rightarrow 1.8 \rightarrow 1.7 \rightarrow 1.6$$

The significant point is that this dependence is the same as for the d.c. conductivity.

5. Time-domain measurements

The dielectric response of a material may be fully characterized in one of two equivalent ways – subject only to the condition of linearity of

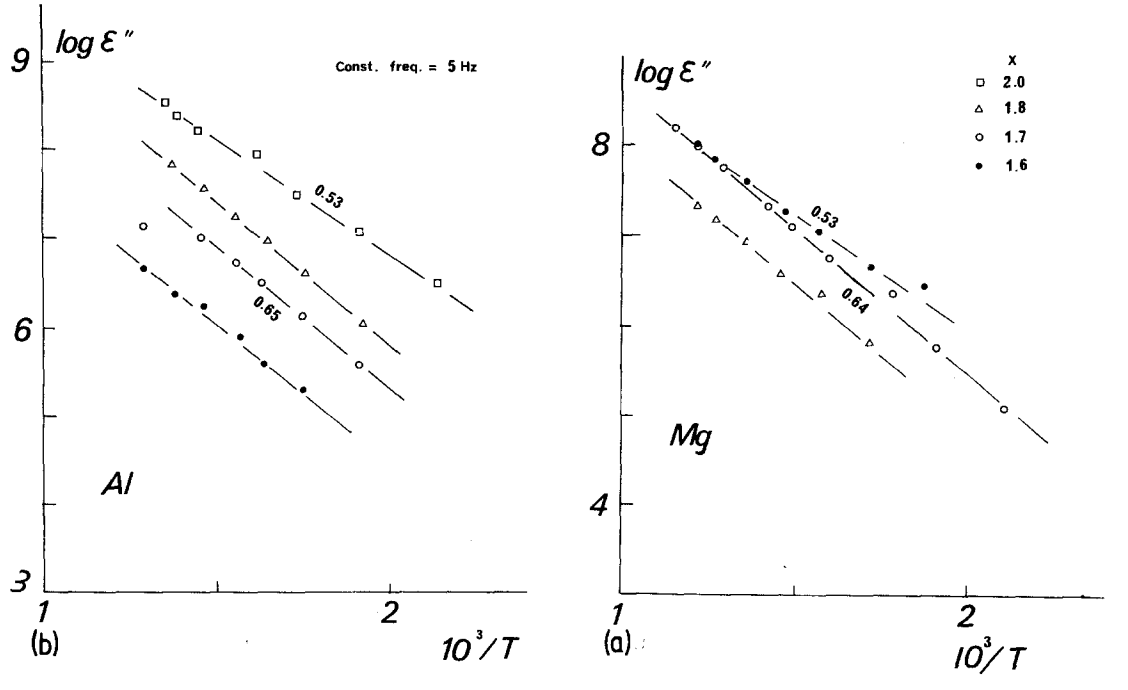

Figure 9 The activation plots of the loss at the lowest frequency of 5 Hz against the reciprocal temperature for the various compositions in the Al and Mg series. The activation energies appear to be comparable in both series and the spread of values with composition is larger for Al.

response with the amplitude of the applied signal. One of these is the widely used frequency response representation, either as the complex impedance plot or, in our opinion preferably, in terms of the frequency dependence of the real and imaginary components of the complex permittivity. The other method is to plot the time dependence of the charging and discharging currents under step function charging and discharging. The two representations are Fourier transforms of one another.

In an ideal system, the charging and discharging currents should differ by a constant magnitude of the direct current, i_0. However, in non-ideal systems it is well known that the difference between the charging and discharging currents is not a constant and this provides the evidence for some non-linear processes [7].

Very few measurements have been reported on any ionic conductors in the time domain and this is regrettable, since this manner of investigation gives a much more immediate evidence of non-linearities than the more common frequency domain representation. We report here one result for $K_2MgTi_7O_{16}$, beginning with 10^{-4} sec after the onset of the step function and extending over some eight decades of time (Fig. 10).

It is evident that the difference between the two currents is not a constant, but we shall not enter into further details of this phenomenon. The most characteristic feature of the response is the very long flat "tail" of the discharge current – which may be expressed as a time dependence of the type t^{-n}, with a small value of the exponent n. This is exactly the counterpart of the frequency-domain dispersion at low frequencies shown in Figs. 7 and 8. In fact, by analysing the complete time response into two components as indicated in Fig. 10, with the values of the exponent n corresponding to 0.64 at short times, i.e. at high frequencies, and 0.125 at long times or low frequencies, we note that we are able to obtain a Fourier transformed loss characteristic that is very similar to those shown in Fig. 5, except that it relates to a much lower temperature and extends to lower frequencies.

6. Interpretation and conclusions

Our experimental data for the range of hollandite materials show an unusually large span of different types of dielectric response for any single class of materials. It is possible to identify clearly the low-temperature response which is of the classical "universal" type at the lowest temperatures and

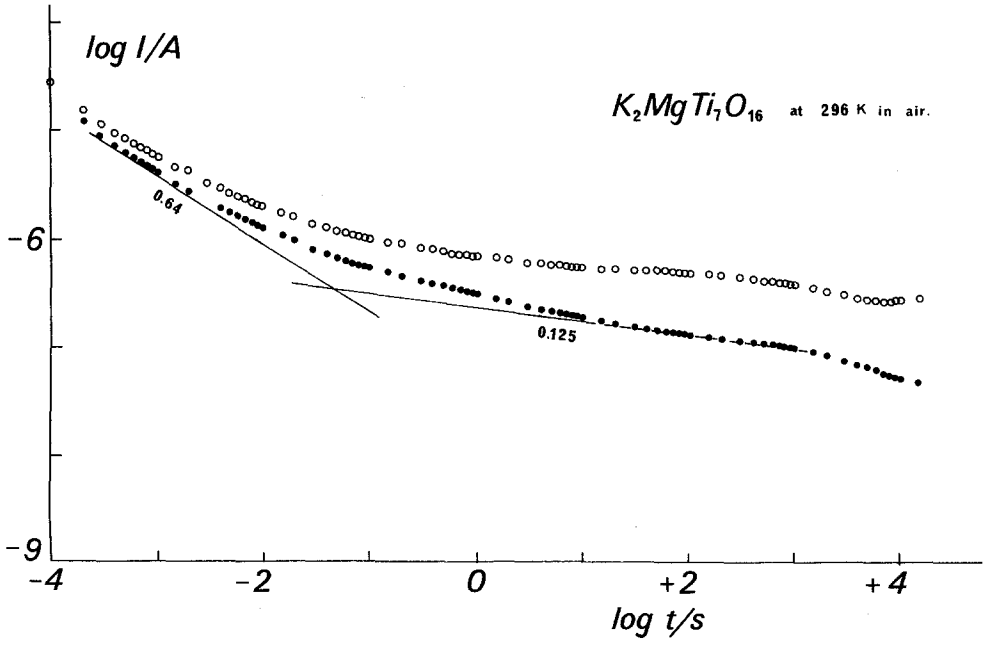

Figure 10 The time-domain response to step function charging and short-circuiting, plotting the logarithm of the charging current $i_c(t)$ (○) and of the discharging current $i_d(t)$ (●) against the logarithm of time. The data relate to $K_2MgTi_7O_{16}$ at 296 K and they were obtained using an automatic digital current measuring equipment constructed by J. T. Ryan under an SRC Research Grant [17]. The two straight lines represent an attempt to fit the data to two Curie–von Schweidler laws of the form $i_d(t) \propto t^{-n}$ with the given values of the exponents n. The difference between $i_c(t)$ and $i_d(t)$ is not a constant, indicating some non-linearity in the system.

becomes overshadowed by a dipolar mechanism at intermediate temperatures. The universal response shows a very weak temperature dependence, which is a common feature of many such responses and the dipolar loss peak response gives the familiar frequency dependence with a low activation energy of the order 0.1 to 0.2 eV.

We propose to identify the response at 77 K with the localized movements of ionic charge carriers over very short distances, almost certainly along the one-dimensional tunnels of easy flow. These are many-body interactions on account of the high densities of the mobile species, but their contribution to direct current conduction is negligible at the low temperatures in question. This interpretation in terms of movements of charge carriers is based on the absence of any loss peak down to the lowest frequencies investigated [7]. The value of the "high-frequency" dielectric permittivity at this temperature appears to be of the order of 60 to 80 which is reasonable for this type of material.

The onset of the clearly observable loss peak in both series of samples at temperatures in the range 120 to 170 K must be related to a "dipolar" process. Taking into account the oxygen environment of the potassium ions this could be interpreted as vibrations of the K–O bonds. We are dealing with a high density of dipolar species, as is witnessed by the resulting large increment of ϵ' – approximately one order of magnitude – in comparison with the first mechanism.

It is interesting to note here that the Al series shows a stronger loss peak amplitude than does the Mg series (Fig. 3). This result could be explained by the fact that the K–O bonds are weaker in the Al solutions [12] on account of the more covalent character of the Al–O bond in comparison with the Mg–O bond.

It is significant that the dependence on x does not reflect the same trend as the d.c. conductivity and the strongly dispersive region, suggesting that the two sets of phenomena are quite different in nature. The highly dispersive behaviour observed in the region of temperatures in excess of some 500 K represents an entirely different feature of the behaviour of hollandites, distinguishing them from the majority of other fast ion conductors. This dispersion is found in many materials the common feature of which is the presence of large densities of mobile charge carriers [16]. Its proposed interpretation invokes the concept of strongly interacting dipoles created by charge carriers which are restricted to movements in localized regions – in the case of hollandites it is proposed that these are the spaces between "blocking" defects in channels (Fig. 11). The fact that this type of dispersion obeys the Kramers–Kronig relations proves that it is a volume effect which is linear in the applied electric field and that it is not the question of some blocking action at electrodes or at grain boundaries. However, unlike the many-body interactions governing the low-temperature dielectric response, this mechanism is closely related to the d.c. conductivity, both as regards the magnitude of the activation energy and with respect to its dependence on the composition fraction x.

Having reached a "lattice" response at sufficiently low temperatures, we may then raise the temperature and watch the onset of the high values of permittivity. If this sets in gradually with increasing temperature, there is every reason to believe that this is a bulk effect manifesting itself as the carrier "mobility" increases. The presence of a barrier would be expected to result in a much more rapid onset of barrier phenomena which depend on the densities of charge carriers rather than on their mobility – usually a more strongly activated process.

We conclude the present discussion with the remark that our entire interpretation of the very interesting and varied dielectric response of

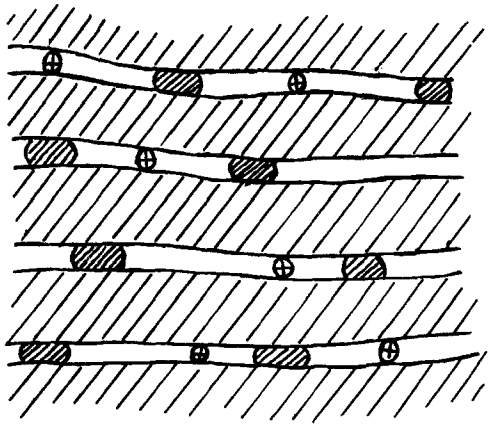

Figure 11 The proposed nature of the "giant dipoles" in the hollandite structure, resulting from the presence of point defects blocking the one-dimensional channels at random intervals. The potassium ions K^+ are, therefore, constrained to move in strictly limited regions, unless they receive sufficient thermal energy to overcome the blocking action. The interaction of these giant dipoles gives rise to the strong low-frequency dispersion.

hollandites is placed in the framework of the "universal" dielectric response. This involves many-body interactions which lead to departing drastically from the classical Debye responses [18]. We believe that the present approach is satisfying in that it offers an explanation of the observed phenomena in terms of simple concepts of universal applicability.

Note added in proof

Most recent measurements on sample Mg, $x = 1.6$, reveal that ϵ' and ϵ'' change very little between 77 and 5.2 K [19], confirming the non-activated many-body nature of the phenomena in question.

Acknowledgements

We are indebted to Mr J. Pugh for his help with the numerical display and plotting of data and to Mr J. T. Ryan for the current measurements on the equipment developed by him. Financial support from the Science Research Council is acknowledged. One of us (K.L.D.) wishes to acknowledge grant support from the Government of India.

References

1. G. D. MAHAN and W. L. ROTH, Eds., "Superionic Conductors" (Plenum Press, New York, 1976).
2. M. KLEITZ and J. DUPUY, Eds., "Electrode Processes in Solid State Ionics" (Reidel, Dordrecht, 1976).
3. R. A. HUGGINS and I. D. RAISTRICK, Workshop on Advanced Battery Design and Research, March (1976).
4. Y. DANTO, G. POUJADE, J. D. PISTRÉ, C. LUCAT and J. SALARDENNE, *Thin Solid Films* (in press).
5. A. K. JONSCHER, *Nature* **267** (1977) 673.
6. *Idem, J. Mater. Sci.* **13** (1978) 553.
7. *Idem,* "The Universal Dielectric Response, A Review of Data and their New Interpretation," (Chelsea Dielectrics Group, 1978).
8. *Idem, Thin Solid Films* **50** (1978) 187.
9. A. K. JONSCHER and J.-M. RÉAU, *J. Mater. Sci.* **13** (1978) 563.
10. A. D. YOFFE, *Chem. Soc. Rev.* **5** (1978) 51.
11. J.-M. RÉAU, J. MOALI and P. HAGENMULLER, *Compt. Rend. Acad. Sci. Paris* **284** (1977) C-655.
12. *Idem, J. Phys. Chem. Solids* **38** (1977) 1395.
13. D. D. ELEY, *J. Polymer Sci. C Polymer Symp.* **17** (1967) 73.
14. A. K. JONSCHER, *Phys. Stat. Sol. (b)* **83** (1977) 585; **84** (1977) 159.
15. C. T. MORSE, *J. Phys. E: Sci Instrum.* **7** (1974) 657.
16. A. K. JONSCHER, *Phil. Mag. B* **33** (1978).
17. J. T. RYAN, SRC Progress Report, November 1977, Chelsea Dielectrics Group
18. K.-L. NGAI, A. K. JONSCHER and C. T. WHITE. *Nature* **277** (1979) 185.
19. K. L. DEORI and A. K. JONSCHER, *J. Phys. C: Solid State Phys.* (in press).

Received 19 July and accepted 13 October 1978.